Case Study of Application of FRP Composites in Strengthening the Reinforced Concrete Headstock of a Bridge Structure

Abolghasem Nezamian[1] and Sujeeva Setunge[2]

Abstract: Worldwide interest is being generated in the use of fiber-reinforced polymer composites (FRP) in the rehabilitation of aged or damaged reinforced concrete structures. As a replacement for the traditional steel plates or external posttensioning in strengthening applications, various types of FRP plates, with their high strength-to-weight ratio and good resistance to corrosion, represent a class of ideal material in externally retrofitting. This paper describes a solution proposed to strengthen the damaged reinforced concrete headstock of the Tenthill Creeks Bridge, Queensland, Australia, using FRP composites. A decision was made to consider strengthening the headstock using bonded carbon FRP laminates to increase the load carrying capacity of the headstock in shear and bending. The relevant guidelines and design recommendations were compared and adopted in accordance with AS 3600 and Austroads bridge design code to estimate the shear and flexural capacity of a rectangular cracked FRP reinforced concrete section.

DOI: 10.1061/(ASCE)1090-0268(2007)11:5(531)

CE Database subject headings: Concrete, reinforced; Bridges, concrete; Shear strength; Case reports.

Introduction

Rehabilitation and upgrading of existing civil engineering infrastructure has recently become a major issue that often requires immediate attention of asset managers. There are a number of situations where an increase in structural capacity or rehabilitation of a bridge structure is required due to environment effects, overloads, aging, design, and construction errors. Costs of repair and/or replacement of the deficient structures are continuously rising. Even when resources are available, extended time is often required for performing needed remedies, causing distribution of traffic and inconvenience to the traveling public. Most of these bridges have older design features that prevent them from accommodating current traffic volumes with modern vehicle sizes and weights. Traditional repair, strengthening, or replacement of bridge components to resist higher design loads, correct deterioration-related damage, or increase ductility has been accomplished using conventional materials and construction techniques. Externally bonded steel plates, steel or concrete jackets, and external post tensioning are just some of the many traditional techniques available. Recent developments in fiber-reinforced polymer (FRP) composites have opened up a cost-efficient alternative for rehabilitation and strengthening of the aged concrete structures (Nezamian et al. 2004a,b). Strength of FRP composites come largely from the fibers, which are usually glass, carbon, or aramid. FRP materials are lightweight, noncorrosive, nonmagnetic and exhibit high tensile strength. Additionally, these materials are readily available in several forms ranging from factory made laminates to dry fiber sheets that can be wrapped to conform to the geometry of a structure before adding the polymer resin. The relatively thin profile of cured FRP systems is often desirable in applications where aesthetics or access is a concern (Nystrom et al. 2003).

FRP systems can be used to rehabilitate or restore the strength of a deteriorated structural member, or retrofit or strengthen a sound structural member to resist increased loads due to changes in use of the structure, or address design or construction errors. Due to the characteristics of FRP materials, behavior of FRP strengthened members, and various issues regarding the use of externally bonded reinforcement, specific guidance on the use of these systems is needed in accordance with the Australian design standards. Although there have been a number of reinforced concrete bridge strengthening projects completed in Australia using FRP materials, in each instance, an overseas consulting company or an academic institution has been used to perform the structural design and consultancy advice using different design guidelines (Kalra and Neubauer 2003; Shepherd and Sarkady 2002).

This paper covers a case study of strengthening of the deteriorated Tenthill Creek Bridge headstock in Queensland using FRP composites. The relevant guidelines and design recommendations were adopted for the headstock in accordance with AS3600 (2002) and the Austroads Bridge Design Code (1992) to estimate the shear and flexural capacity of a rectangular reinforced concrete section strengthened with FRP reinforcement. This paper also aims to compare and review the recommendations and contents of the available guidelines in the context of the design of an externally bonded FRP system for flexural and shear strengthening of a reinforced concrete bridge headstock.

[1]Postdoctoral Research Fellow of CRC Construction Innovation, School of Civil and Chemical Engineering, RMIT Univ., City Campus, Melbourne VIC 3001, Australia. E-mail: abe.nezamian@rmit.edu.au

[2]Senior Lecturer of School of Civil and Chemical Engineering, RMIT Univ., City Campus, Melbourne VIC 3001, Australia. E-mail: sujeeva.setunge.rmit.edu.au

Note. Discussion open until March 1, 2008. Separate discussions must be submitted for individual papers. To extend the closing date by one month, a written request must be filed with the ASCE Managing Editor. The manuscript for this paper was submitted for review and possible publication on August 13, 2004; approved on October 6, 2005. This paper is part of the ***Journal of Composites for Construction***, Vol. 11, No. 5, October 1, 2007. ©ASCE, ISSN 1090-0268/2007/5-531–544/$25.00.

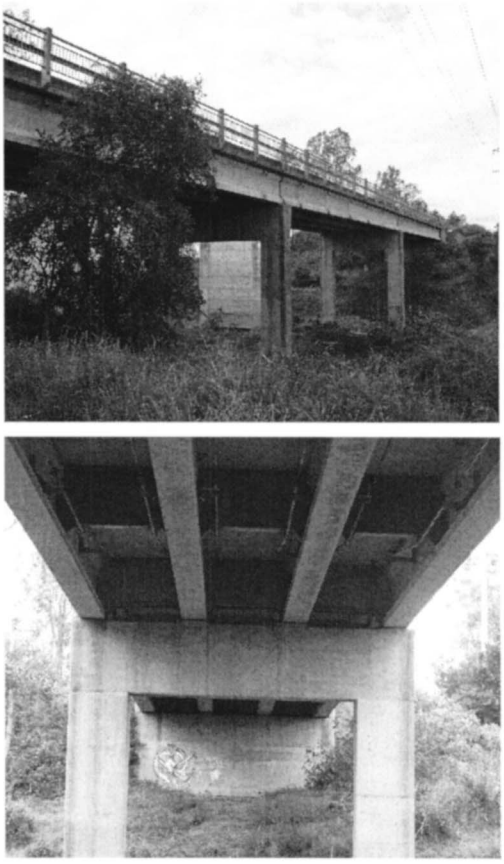

Fig. 1. Photos of Tenthill Bridge

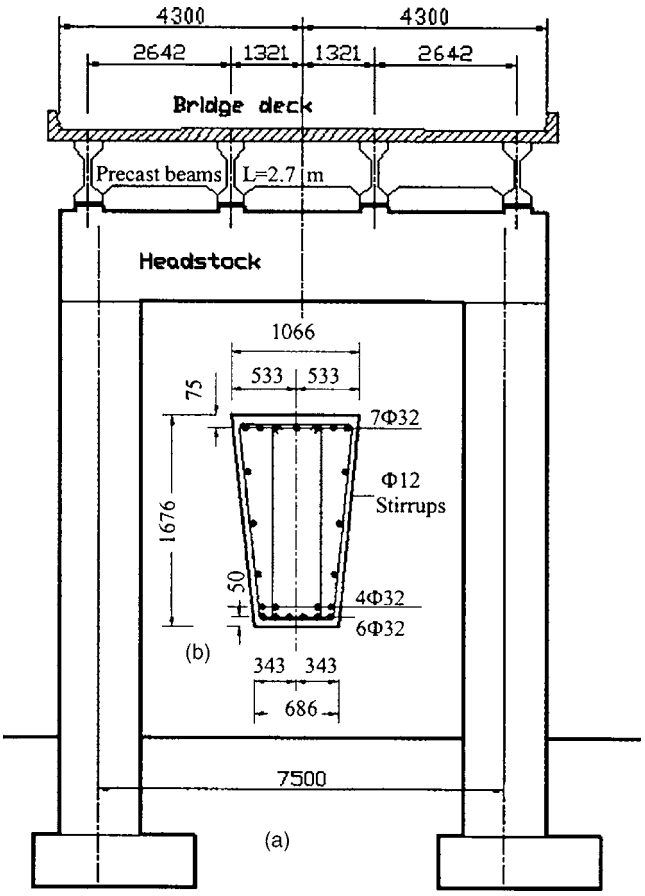

Fig. 2. (a) Schematic view; (b) cross section of the headstock

Description of the Case Study

The bridge studied in this report carries Gatton Helidon Rd. over Tenthill Creek in Gatton, Queensland, Australia. This simple three span reinforced concrete, prestressed beam structure was built in the 1970s. The bridge is 82.15 m long and about 8.6 m wide and is supported by a total of 12 prestressed 27.38 m long beams over three spans of 27.38 m. Side and cross views of the Tenthhill Bridge are shown in Fig. 1. The beams are supported by two abutments and two headstocks. A headstock elevation view is shown in Fig. 2.

Preliminary Structural Assessment

Queensland Department of Main Roads (QDMR) has a comprehensive asset management system of inspections, condition data, analysis and prioritization tools, maintenance manuals, and heavy load routing systems (Fenwick and Rotolone 2003). The asset management system aims to maintain the bridges in a condition that allows heavy vehicles free access to all parts of the network by avoiding load restrictions on any bridge in the primary (state-controlled roads) network. The Tenthill Bridge has been observed to require immediate strengthening to avoid such restriction. The overall evaluation included a thorough field inspection, review of the existing design or as-built documents, and a structural capacity analysis in accordance with AS3600 (2002) and the Austroads Bridge Design Code (1992). Existing construction and operational documents for the bridges were reviewed, including the design drawings, project specifications, as-built information, and past repair documentation. The Austroads Bridge Design Code (1992) was used for assessment of the bridge to ascertain the capacity of the bridge. The Gatton-Helidon Rd. over Tenthill Creek is selected as functional Class 3 from Table 2.3.4 of the Austroads Code (1992). The Road Class 3 main function is to form an average of communication for movements between important centers or key towns. Hence, the heavy load platform HLP 320 design loading shall be applied on the bridge.

Observed Cracks

The bridge has two headstocks supporting the prestressed concrete beams. In the first headstock, only flexural cracking was observed, whereas in the second headstock, both flexural cracking and shear cracking were observed. A maximum flexural crack width of 0.6 mm and a shear crack width of 2.8 mm was reported. A photograph of the damaged headstock and a schematic of the cracked beam are shown in Fig. 3.

Structural Analysis

The headstock was analyzed as a portal frame considering all necessary design situations and load combinations according to the Austroads Bridge Code (1992) for ultimate and serviceability limit states. The grillage analysis (lane analysis) was used to calculate traffic load effects on the headstock. The traffic loading models of T44 truck loading and heavy load Platform loading of HLP 320 in one and two lanes were used in the grillage analysis (Fig. 4). The computer program Space Gass was used by QDMR for structural analysis and the research team used the SAP 2000 (CSi Products 2003) computer program to check the structural

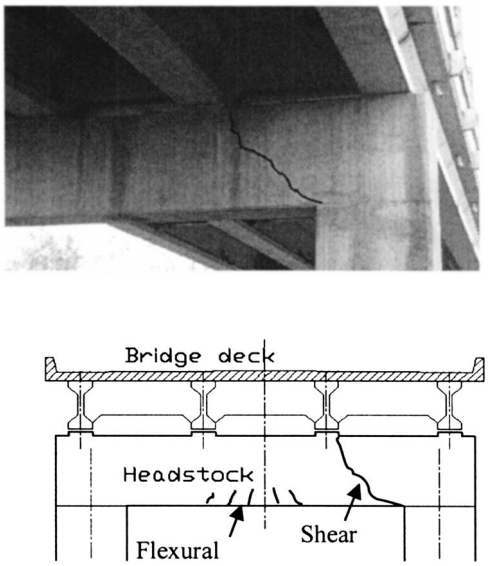

Fig. 3. Observed cracks in the headstock

analysis. After consulting with QDMR, it was decided to set the strengthening target for the ultimate bending moment and shear force that resulted from the combination of ultimate traffic loads using T44 traffic loading and permanent effect (dead load). The load carrying capacity of the bridge would then be consistent with the other bridges in that part of the network. The ultimate positive bending moment of 5,320 kN m in midspan, ultimate shear force of 2,520 kN, serviceability bending moment of 2,526 kN m and serviceability shear force of 1,797 kN were then calculated using this load combination. Load factors and combinations are summarized in Table 1.

Existing Capacity of Beam in Frame Bent (Headstock)

In accordance with the Australian codes of practice for structural design, the capacity analysis methods contained in this section are based on ultimate limit-state philosophy. This ensures that a member will not become unfit for its intended use and its design strength is not less than the design action according to the provisions of the Australian standard for concrete structures AS3600 (2002). The capacity analysis results would be compared with structural analysis results to identify the deficiencies.

A typical beam section of the headstock is shown in Fig. 2. The positive and negative flexural and shear capacities of the section were calculated in accordance with the Australian standards AS3600 (2002). The nominal steel reinforcing bar areas, nominal steel yield strength of 400 MPa for longitudinal reinforcement and 240 MPa for shear reinforcement, and nominal concrete compressive strength of 20 MPa were used in the section capacity analysis. The positive residual flexural capacity of 3,840 kN m at midspan was then calculated for the beam in accordance with the Austroads Bridge Design Code (1992, Clause 5.8.1.2). The capacity was calculated using a rectangular stress block where the neutral axis lies within the cross section, provided that the maximum strain in the extreme compression fiber of the concrete is taken as 0.003. Based on structural analysis, the residual negative flexural strength is adequate for the applied negative bending moment and no strengthening is required. The residual shear capacity of 2,065 kN was also calculated for the

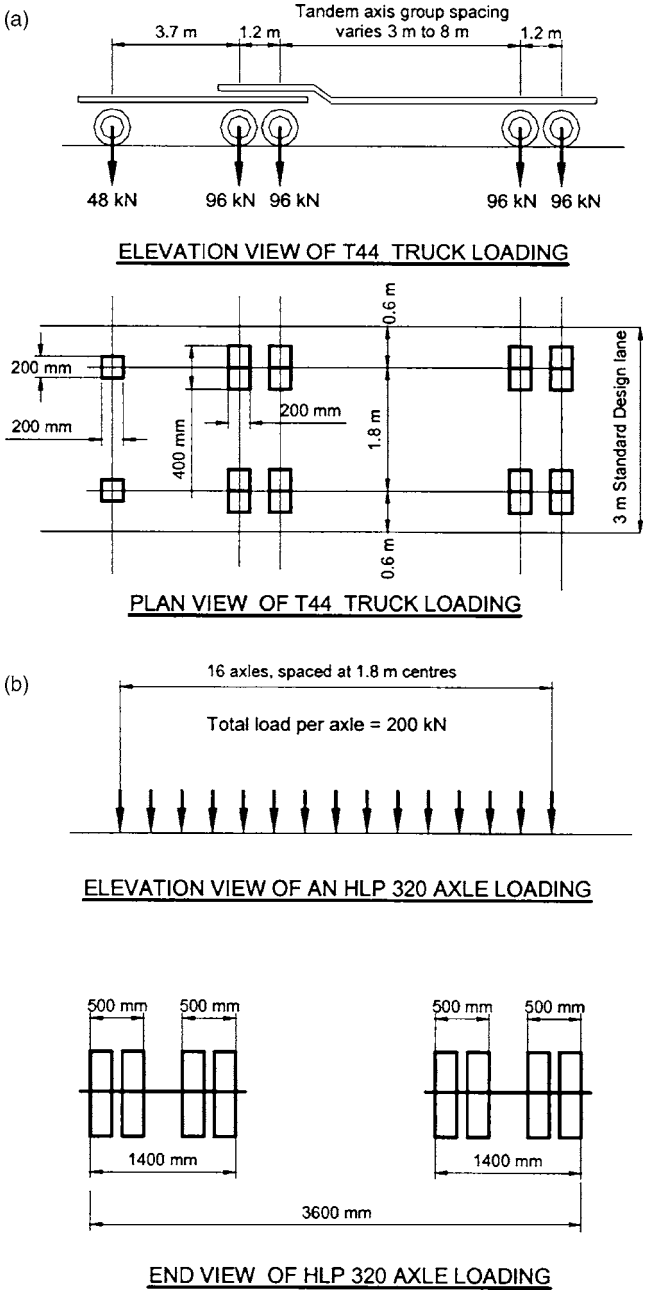

Fig. 4. (a) T44 Truck loading; (b) lateral spacing of dual wheels along an axle for heavy load platform loading

beam according to Clauses 5.8.1.3 and 5.8.2 of the Austroads Bridge Design Code (1992) by means of a method based on truss analogy, using the following equations:

$$V_u = V_{uc} + V_{us} \tag{1}$$

where V_u=ultimate shear strength; V_{uc}=ultimate shear strength excluding shear reinforcement; and V_{us}=contribution by the shear reinforcement to the ultimate shear strength:

$$V_{uc} = \beta_1\beta_2\beta_3 b_v d_0 \left(\frac{A_{st} f'_c}{b d_0}\right)^{1/3} \tag{2}$$

where

$$\beta_1 = 1.1(1.6 - d_0/1000) \geq 1.1 \tag{3}$$

β_2=1 or

Table 1. Load Factors and Combinations

State of design	Load combinations
Limit state	1.25DL+2.8T44+Ulimate flood (3 combinations)
Limit state	1.25DL+2.8T44 (2 lanes)+Ulimate flood
Limit state	1.25DL+2.8Truck T44
Limit state	1.25DL+2.8×2Truck T44 (2 lanes)
Limit state	1.25DL(flood)+Ulimate Flood (3 combinations)
Serviceability	1.0DL+1.4Truck T44
Serviceability	1.0DL+1.4×2Truck T44 (2 lanes)
Serviceability	1.0DL (flood)+Flood (3 combinations)
Serviceability	1.0DL (flood)+1.4 T44+Flood
Serviceability	1.0DL (flood)+1.4×T44 (2 lanes)+Flood

$$\beta_2 = 1 - (N^*/3.5A_g) \geqslant 1 \text{ for members subject to significant axial tension; or} \quad (4)$$

$$\beta_2 = 1 + (N^*/14A_g) \text{ for the members subject to significant axial compression} \quad (5)$$

$\beta_3=1$ or may be taken as $2d_0/a_v$ but not greater than 2, provided that the applied loads and the support are oriented so as to create diagonal compression over the length a_v. A_{st}=cross section of longitudinal reinforcement provided in the tension zone and fully anchored at the cross section under consideration; b=effective width of a web for shear, and d_0=distance from the extreme compression fiber of the concrete to the centroid of the outermost layer of tensile reinforcement. Although the calculated applied bending moments and shear force in serviceability limit state are relatively lower than the structural capacity of the headstock, a decision was made to strengthen the headstock for ultimate bending moments and shear and to contain the cracking.

FRP Strengthening of the Headstock

After the preliminary analysis, it was decided to develop an innovative solution using FRP composites for strengthening. The details of the calculations are given in this paper, identifying the decisions faced by the designer at various stages of the development of the innovative solution. The applicability of FRP composites to concrete structure for rehabilitation or capacity enhancement has been actively studied in numerous research laboratories and professional organizations around the world (ACI 2003, International 2002; Bakis et al. 2002; JSCE 1997; Bakht et al. 2000; Pantelaides et al. 2004b). There are also many examples of documented retrofits of older reinforced concrete bridges and other structures with FRP composites (Seible et al. 1995; Policelli 1995; Shahrooz and Boy 2004; Pantelides et al. 2004a). FRP reinforcements offer a number of advantages such as corrosion resistance, nonmagnetic properties, high tensile strength, and light weight and ease of handling.

Design Guidelines

As the use of FRP composites for strengthening of reinforced concrete structures is a relatively new technique, the development of design guidelines for externally bonded FRP systems is ongoing in Europe, Japan, Canada, and the United States. Within the last 10 years, many design guidelines have been published to provide guidance for the selection, design, and installation of FRP systems for external strengthening of concrete structures. In Europe, Task Group 9.3 of the International Federation for Structural Concrete published *Bulletin 14* (FIB 14) on design guidelines for externally bonded FRP reinforcement for reinforced concrete structures. In the United States, ACI Committee 440 (2003) developed a guide for the design and construction of externally bonded systems or strengthening concrete structures.

Table 2. Material Properties of the Sika CFRP Systems

Type	Tensile strength (MPa)	Elastic modulus (MPa)	Elongation at break (%)
CarboDur Type S	2,800	165,000	1.7
Sika-Wrap 230C	3,500	230,000	1.5

Design of FRP System

All necessary design situations and load combinations were considered, which were already outlined. The nominal strength of a member is assessed based on the possible failure modes and subsequent strains and stresses in each material. It was decided to bond FRP laminates to the tension face of the beam section (bottom fiber) of the frame with fibers oriented along the length of the member for positive flexural strengthening and use a complete wrapping scheme with fibers oriented transversely for the shear strengthening. After consulting with suppliers of FRP materials in Australia, it was decided to use Sika CFRP laminate CarboDur Type S for flexural strengthening and Sika CFRP wet lay up type Sika-Wrap-230C, Sika Australia Pty (2004), Melbourne, Australia. Table 2 shows material properties of proposed systems. The Sika CFRP materials can be replaced by similar MBT CFRP products of MBrace CFK laminate 150/2,000 for flexural and MBrace CF 130 for shear strengthening, MBT Australia Ltd, Melbourne, Australia. Table 3 shows material properties of the proposed MBrace systems. However, a choice between the manufacturers has not been considered in terms of application and installation of the FRP strengthening systems.

Flexural Strengthening

In the analysis for the ultimate state in flexure, both design guidelines follow well established procedures using idealized stress–strain curves for concrete, FRP, and longitudinal reinforcement (see Fig. 5). These curves, along with the following assumptions, form the basis for the ultimate strength limit state analysis of a concrete element strengthened in flexure.

Table 3. Material Properties of Mbrace CFRP Systems

Type	Tensile strength (MPa)	Elastic modulus (MPa)	Elongation at break (%)
Mbrace CFK Laminates 150/2,000	2,700	165,000	1.4
Mbrace CF 130	3,800	240,000	1.55

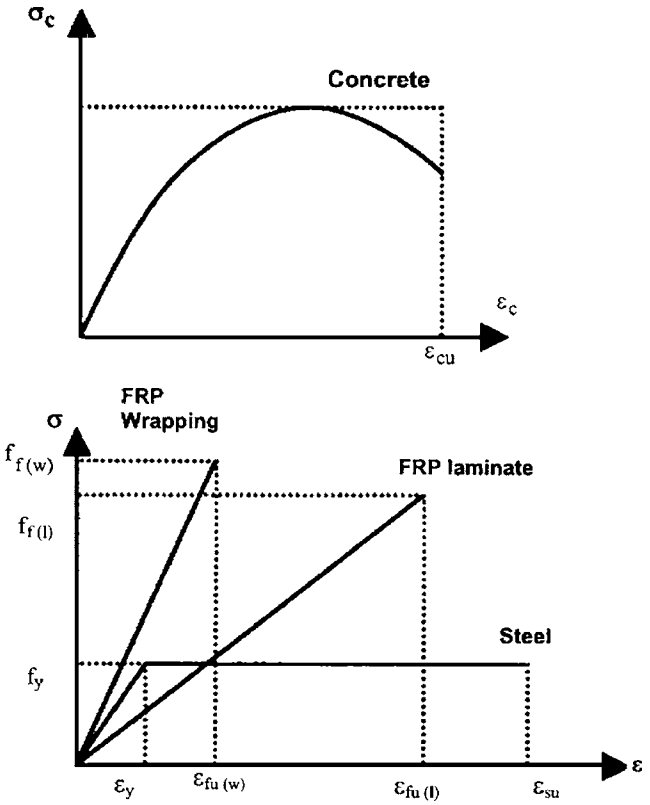

Fig. 5. Idealized stress–strain curves for constitutive materials at ULS

- Design calculations are based on the actual dimensions, internal reinforcing steel arrangement, and material properties of the existing member being strengthened;
- The strains in reinforcement and concrete are directly proportional to the distance from the neutral axis, that is, a plane section before loading, remains plane after loading;
- There is no relative slip between external FRP reinforcement and the concrete; and
- The shear deformation within the adhesive layer can be neglected since the adhesive layer is very thin with slight variations in its thickness.

The cross-sectional analysis identifies all possible failure modes. Failure of the strengthened element may then occur as a result of various mechanisms as follows:

- Crushing of the concrete in compression before yielding of the reinforcing steel;
- Yielding of the steel in tension followed by rupture of the FRP laminates;
- Yielding of the steel in tension followed by concrete crushing;
- Shear/tension delamination of the concrete cover; and
- Debonding of the FRP from the concrete substrate.

Design Material Properties

According to the FIB guideline, the design strength is obtained by dividing the characteristic strength by a partial safety factor. The partial safety factors for concrete (in flexure), γ_{mc}, and steel reinforcement, γ_{ms}, are normally taken as 1.5 and 1.15, respectively. The partial safety factors applied on the characteristic strengths of FRPs are mainly based on the observed differences in the long-term behaviors of FRPs (basically depending on the type of fibers), as well as the application method and on-site working conditions. A partial safety factor for carbon fiber in application type B under difficult on-site working condition, γ_{ms}, of 1.35 is indicated. The design material properties for the headstock according to the FIB guideline are listed in Table 4. The ACI design guideline suggests that the design tensile strength should be determined using the environmental reduction factor only for FRP materials. The reduction factors are mainly based on the types of fiber and environmental conditions. Similarly it is suggested to reduce the design rupture strain for environmental-exposure conditions. A reduction factor for carbon fiber in an aggressive environment, C_E, of 0.85 was used. The design material properties for the headstock according to the ACI guideline are listed in Table 5.

Table 4. Design Material Properties Complying with the FIB Guideline

Material	Design strength (MPa)	Elastic modulus (MPa)	Allowable strain
Concrete	21/1.5=14	26,100[a]	0.0035
Steel bars	400/1.15=348	200,000	0.002
CFRP strips (flexural)	2,800/1.35=2,047	165,000	0.017/1.35=0.0126
CFRP wrapping (shear)	3,500/1.35=2,593	230,000	0.015/1.35=0.0111

[a]Long term modulus of elasticity of 13,050 was used to account for creep of concrete.

Initial Condition

It was noted by both design guidelines that the effect of the initial load prior to strengthening should be considered in the calculation of the stresses and strains based on theory of elasticity and with the service moment acting on the critical beam section during strengthening. The initial strain distribution of the member may then be evaluated and considered in strengthening calculations. As the service bending moment is typically greater than the cracking moment, the calculation is based on a cracked section. The initial strain distribution of the headstock was calculated based on structural analysis for the service loading condition, long-term modulus of elasticity, and the cracked section. The same initial strain distribution was used for the design of strengthening scheme using both design guidelines.

Capacity of Strengthened Beam

The cross-sectional analysis indicated that the failure mode of the beam section of the headstock would be a result of yielding the longitudinal steel reinforcement followed by concrete crushing, while the FRP is intact. This is the most desirable failure mode,

Table 5. Design Material Properties Complying with the ACI Guideline

Material	Design strength (MPa)	Elastic modulus (MPa)	Allowable strain
Concrete	21 (β_1=0.91)	26,100[a]	0.003
Steel bars	400	200,000	0.002
CFRP strips (flexural)	0.85×2,800=2,380	165,000	0.85×0.017=0.01445
CFRP wrapping (shear)	0.85×3,500=2,975	230,000	0.85×0.015=0.01275

[a]The long term modulus of elasticity of 13,050 was used to account for creep of concrete.

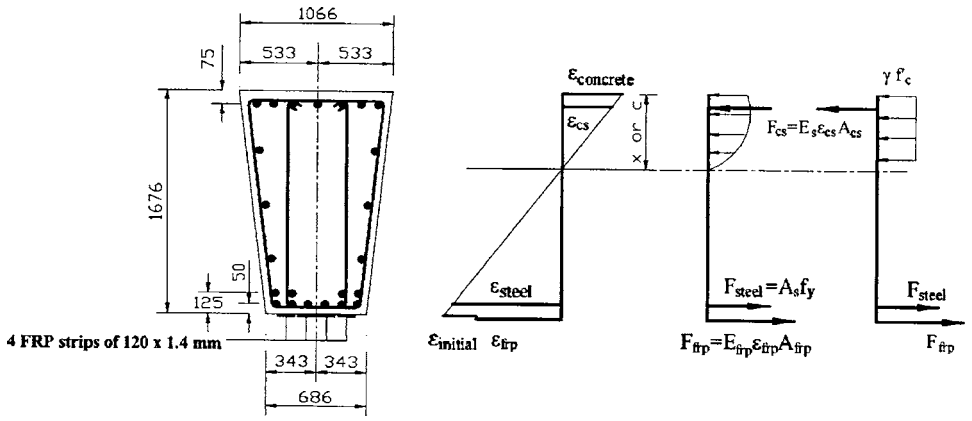

Fig. 6. Internal strain and stress distributions for the beam cross section of the headstock

which satisfies the safety requirements in the ultimate state for a reinforced concrete section. The design bending moment for the strengthened member was then calculated in accordance with each design guideline based on well-established principles of flexural design of reinforced concrete beams. The design principles are shown in Fig. 6. The design positive bending moment capacity of 5,809 and 5,392 kN m were calculated for the strengthened section based on the FIB and ACI design guidelines, respectively. The effect of creep and shrinkage was considered in calculations. Although both design guidelines use the same principles to calculate the capacity of the strengthened member, each design guideline introduces different values for the ultimate strain of the concrete and the strength reduction and material safety factors. The calculated moment capacities using the two design guidelines indicated that the predicted capacity enhancement based on the ACI guideline is more conservative. This is mainly due to the use of an additional strength reduction factor of 0.85 applied to the contribution of FRP reinforcement to flexural capacity enhancement and also higher concrete allowable strain of 0.0035 used in the FIB calculations.

Anchorage

Experimental investigations show that the FRP rupture is a rare event and delamination of FRP strips is more likely to occur before stress in the FRP reaches the ultimate level. Debonding implies the complete loss of composite action between the concrete and FRP laminates. Bond failure will be a brittle failure and should be prevented. The ACI guideline places a limitation on the strain level in the laminate to prevent delamination of FRP from the concrete substrate:

$$\kappa_m = \frac{1}{60\varepsilon_{fu}}\left(\frac{90{,}000}{nE_f t_f}\right) < 0.9 \tag{6}$$

$$\varepsilon_f = \varepsilon_{cu}\frac{h-x}{x} - \varepsilon_0 \leq \kappa_m \varepsilon_{fu} \tag{7}$$

where, κ_m=bond dependant coefficient; ε_{fu}=ultimate FRP strain; E_f=modulus of elasticity of FRP; t_f=thickness of FRP strip; n=number of plies of FRP reinforcement; ε_{cu}=ultimate strain; and ε_0=initial strain at the extreme tensile fiber before strengthening.

The FIB guideline uses a more detailed approach to check the debonding failure. It is noted that the following failure modes need to be considered to prevent delamination of FRP, depending on the starting point of the debonding process.

Debonding in Uncracked Anchorage Zone

This approach involves two independent steps: First, the end anchorage should be verified based on the shear stress–slip constitutive law at the FRP–concrete interface. Then strain limitation should be applied on the FRP to ensure that bond failure far from the anchorage is prevented. The model of Holzenkämpfer (1994) as modified by Neubauer and Rostásy (1997) is used. The maximum FRP force which can be anchored, $N_{fa,\max}$, and the maximum anchorage length, $l_{b,\max}$, can then be calculated (see Fig. 7):

$$N_{fa,\max} = \alpha c_1 k_c k_b b\sqrt{E_f t_f f_{ctm}} \tag{8}$$

$$l_{b,\max} = \sqrt{\frac{E_f t_f}{c_2 f_{ctm}}} \tag{9}$$

where α=reduction factor, approximately equal to 1 in beams with sufficient internal and external shear reinforcement, to account for the influence of reinforcing steel (Neubauer and Rostásy 1997); k_c=factor accounting for the state of compaction of con-

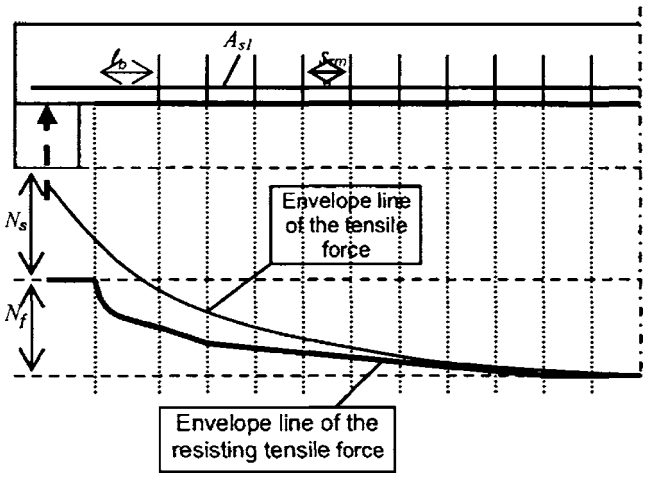

Fig. 7. Envelope line of the total tensile force in FRP and steel reinforcements (International 2002, with permission)

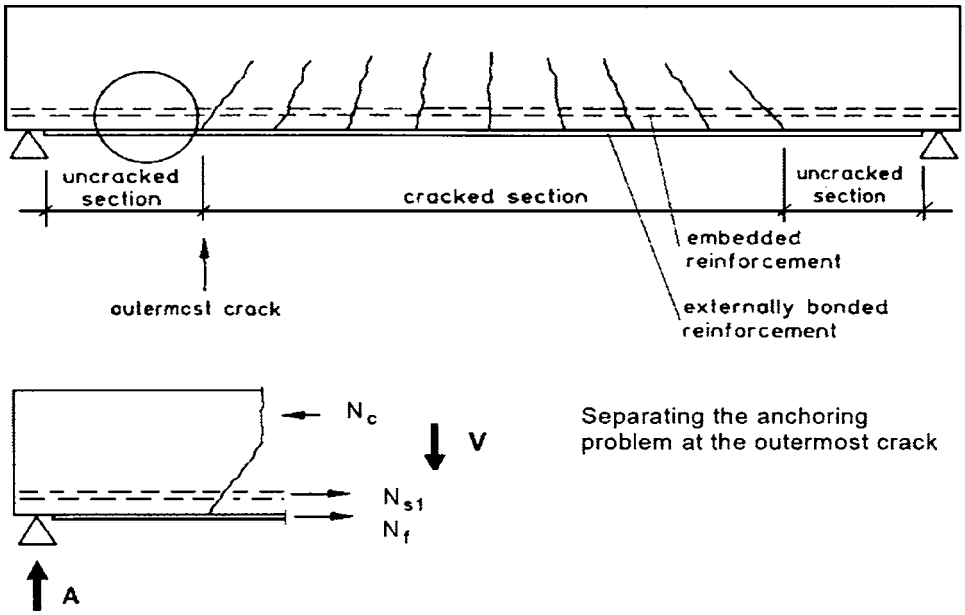

Fig. 8. End anchorage in an uncracked concrete zone (International 2002, with permission)

crete (k_c can generally be assumed to be equal to 1.0); and k_b=geometry factor:

$$k_b = 1.06\sqrt{\frac{2-\frac{b_f}{b}}{1+\frac{b_f}{400}}} \tag{10}$$

c_1 and c_2=0.64 and 2, respectively, for CFRP laminates and f_{ctm}=mean value of the concrete tensile strength. Theoretical cut off point then is calculated using

$$N_{fa,\max} = \frac{M\alpha_f A_f(h-x)}{I_{cs}} \tag{11}$$

where M=applied bending moment at the cutoff point; α_f=modular ratio for nonprestressed steel to the concrete; A_f=total area of FRP reinforcement; and I_{cs}=second moment area of the cracked section. Based on structural analysis (load combination of ultimate HLP 320 and ultimate dead load), the bending moment of 3,985 kN m occurs at 0.65 m from the beam support middle span toward the column. Hence the provided anchorage length of 1.0 m is more than the required end anchorage length of 0.24 m.

Debonding Caused at Flexural Cracks

A more detailed approach to prevent debonding at flexural cracks in case of short-term static loading is proposed by Niedermeier (2000). The aim of this approach is to calculate the maximum possible increase in tensile stress within the FRP strips, which can be transferred by means of bond stresses between two subsequent flexural cracks. This increase should be compared to the increase according to the design assumption of the full composite action. This basic approach consists of three following steps:

- Determination of the most unfavorable spacing of flexural cracks;
- Determination of the tensile force within FRP strip between two subsequent cracks according to the design in bending; and
- Determination of the maximum possible increase in tensile stress in the FRP.

The crack spacing between two subsequent cracks equals approximately two times the transmission length t and may be calculated assuming constant mean bond stresses of both the internal and the external reinforcement using

$$s_{rm} = 2l_t = 2\frac{M_{\text{cr}}}{z_m}\frac{1}{\left(\sum \tau_{fm} b_f + \sum \tau_{sm} d_s \pi\right)} \tag{12}$$

$$z_m = 0.85\frac{(hE_fA_f + dE_sA_{s1})}{(E_fA_f + E_sA_{s1})} \tag{13}$$

$$\tau_{sm} = 1.85 f_{ctm} \tag{14}$$

$$\tau_{fm} = 0.44 f_{ctm} \tag{15}$$

where s_{sm}=mean bond stress of the steel reinforcement; τ_{sm}=mean bond stress of the internal reinforcement; τ_{fm}=mean bond stress of the external reinforcement; M_{cr}=bending moment causing cracking; and d_s=diameter of the steel bars. Constant crack spacing over the whole length of the flexural member may be assumed to simplify the calculation. The tensile stress of the FRP is calculated taking into account the strain compatibility and the internal force equilibrium. The estimated achievable increase in tensile stresses between two subsequent cracks needs to be checked with the tensile stresses as calculated in the flexural design of the beam. The maximum tensile force, which can be transferred from the FRP strips to the concrete by means of bond stresses at the anchorage zone between the cracks, is calculated using the following equations (see Fig. 8) (Niedermier 2000):

$$\max \Delta\sigma_{fd} = \frac{c_3}{\gamma_c}\sqrt{\frac{E_f\sqrt{f_{ck}f_{ctm}}}{t_f}} \tag{16}$$

$$l_{b,\max} = c_4\sqrt{\frac{E_f t_f}{\sqrt{f_{ck}f_{ctm}}}} \tag{17}$$

c_3 and c_4=0.23 and 1.44 for CFRP laminates, respectively, and f_{ck}=characteristic value of the concrete compressive strength. An analysis of the bond behavior of the externally bonded reinforce-

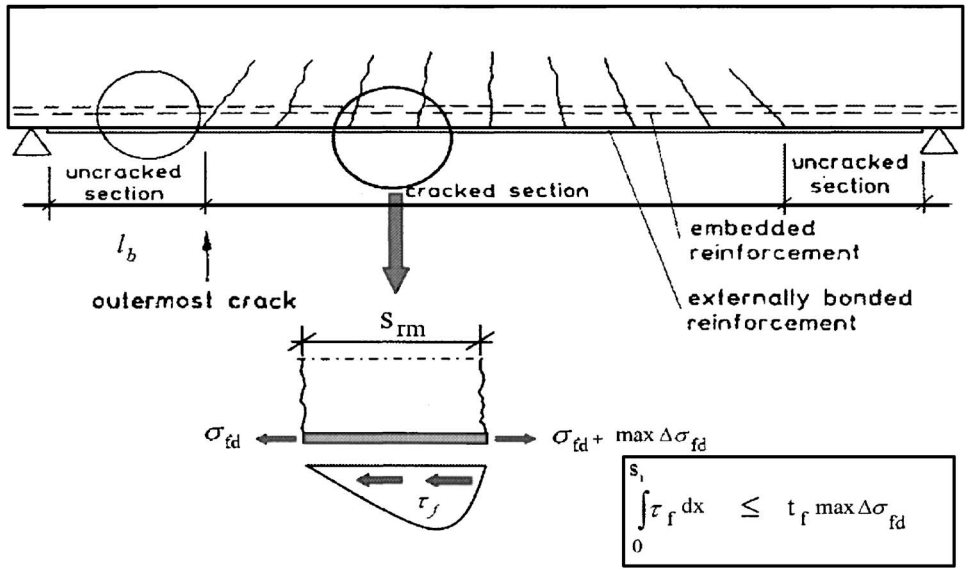

Fig. 9. Element between two subsequent cracks—analysis of debonding at flexural cracks (International 2002, with permission)

ment based on a simplified bilinear bond stress–slip relation can be used to calculate the maximum increase in tensile stress, max $\Delta\sigma_{fd}$, in an element between two cracks depending on the tensile stress $\Delta\sigma_{fd}$, where $\Delta\sigma_{fd}$=tensile stress based on strain compatibility and force equilibrium at the section (Fig. 9). Fig. 10 shows the maximum possible increase for specific crack spacing. Points A, B, and C, shown in Fig. 10 may be estimated using

$$\Delta\sigma_f^{(B)} = \frac{c_5 E_f}{s_{rm}} - c_6\sqrt{f_{ck} f_{ctm}}\frac{s_{rm}}{4t_f} \tag{18}$$

$$\max \Delta\sigma_{fd}^{(B)} = \frac{1}{\gamma_c}\left[\sqrt{\frac{c_1^2 E_f \sqrt{f_{ck} f_{ctm}}}{t_f} + (\sigma_f^{(B)})^2} - \sigma_f^{(B)}\right] \tag{19}$$

where c_5 and c_6=0.185 and 0.285, the linear increase between Points A and B can then be described by Eq. (14) and the graph between B and C is described by

$$\max \Delta\sigma_{fd}^{(1)} = \max \Delta\sigma_{fd}^{(A)} - \frac{(\max \Delta\sigma_{fd}^{(A)} - \max \Delta\sigma_{fd}^{(B)})}{\sigma_f^{(B)}}\sigma_{fd} \tag{20}$$

$$\max \Delta\sigma_{fd}^{(2)} = \frac{1}{\gamma_c}\left[\sqrt{\frac{c_3^2 E_f \sqrt{f_{ck} f_{ctm}}}{t_f} + \sigma_{fd}^2} - \sigma_{fd}\right] \tag{21}$$

For high tensile stress, the upper limit of the increase in stresses is determined by the tensile strength of the FRP:

$$\max \Delta\sigma_{fd}^{(3)} = f_{fd} - \sigma_{fd} \tag{22}$$

The units for Eqs. (8)–(22) are megaPascals for stress and modulus of elasticity and millimeters for dimensions.

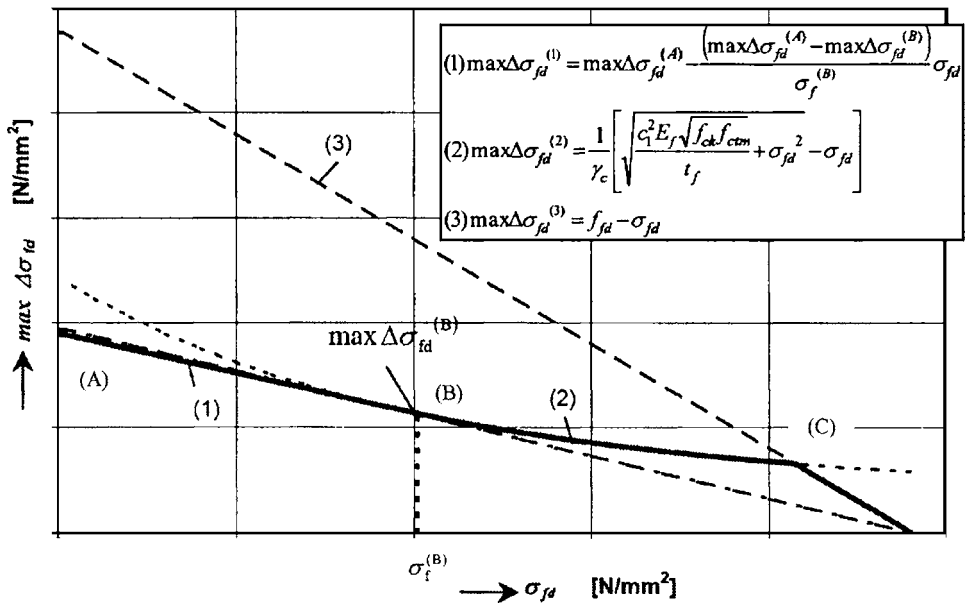

Fig. 10. Diagram of the maximum possible increase in tensile stress between two subsequent cracks (Niedermeier 2000, with permission)

Debonding Caused at Shear Cracks

The end anchorage has already been checked. It should be then checked that the resulted shear stress τ_b from the change of tensile force along the FRP at the FRP–concrete interface is limited (CEB-FIB 2002):

$$f_{cbd} = 1.8\frac{f_{ctk}}{\gamma_c} \tag{23}$$

$$\varepsilon_{s1} < \varepsilon_{yd}: \quad \frac{V_d}{0.95db_f\left(1 + \frac{A_{s1}E_s}{A_fE_f}\right)} < f_{cbd} \tag{24}$$

$$\varepsilon_{s1} \geqslant \varepsilon_{yd}: \quad \frac{V_d}{\frac{z_s + z_f}{2}b_f} < f_{cbd} \tag{25}$$

where f_{cbd}=design bond shear strength of concrete; f_{ctk}=characteristic value of the concrete tensile strength; V_d=max shear force; z_s and z_f=lever arms of internal forces for longitudinal and FRP reinforcements. Due to the substantial width of the bond interface available, the previous verification is not critical. Debonding of CFRP strips was checked based on each guideline and the calculations indicated that the strengthening system satisfies the requirements from both guidelines to prevent the debonding failure. It appears that the FIB guideline uses a more involved methodology to check the debonding failure, considering all possible failure modes. However the debonding failure of CFRP strips in the strengthening of the headstock will be also controlled by applying CFRP wrapping scheme for shear strengthening (see Figs.)

Shear Strengthening

The design for shear strengthening of a reinforced concrete member in both guidelines is based on truss model and superposition principle with some considerations for the orthotropic behavior of the CFRP material. The shear strength of a strengthened member is determined by adding the contribution of the CFRP reinforcing to the contributions from the concrete and shear reinforcement:

$$V_{\text{total}} = V_{uc} + V_{us} + V_{\text{frp}} \tag{26}$$

where V_{uc}, V_{us}, and V_{frp}=contributions from the concrete, steel and the FRP, respectively.

According to the ACI guideline the shear strength should be calculated using the strength-reduction factor, ϕ, required by ACI 318-99 (1999)

$$\phi V_n \geqslant V_u \tag{27}$$

The nominal shear strength of a FRP-strengthened concrete member can be determined by adding the contribution of the FRP reinforcement to the contributions from the shear steel reinforcement and the concrete. It is also suggested that an additional reduction factor of ψ_f=0.95, be applied to the shear contribution of the FRP reinforcement:

$$\phi V_n = \phi(V_{uc} + V_{us} + \psi_f V_{\text{frp}}) \tag{28}$$

$$V_{\text{frp}} = \frac{A_{fv}f_{fe}(\sin\alpha + \cos\alpha)d_f}{S_f} \tag{29}$$

$$f_{fe} = \varepsilon_{fe}E_f \tag{30}$$

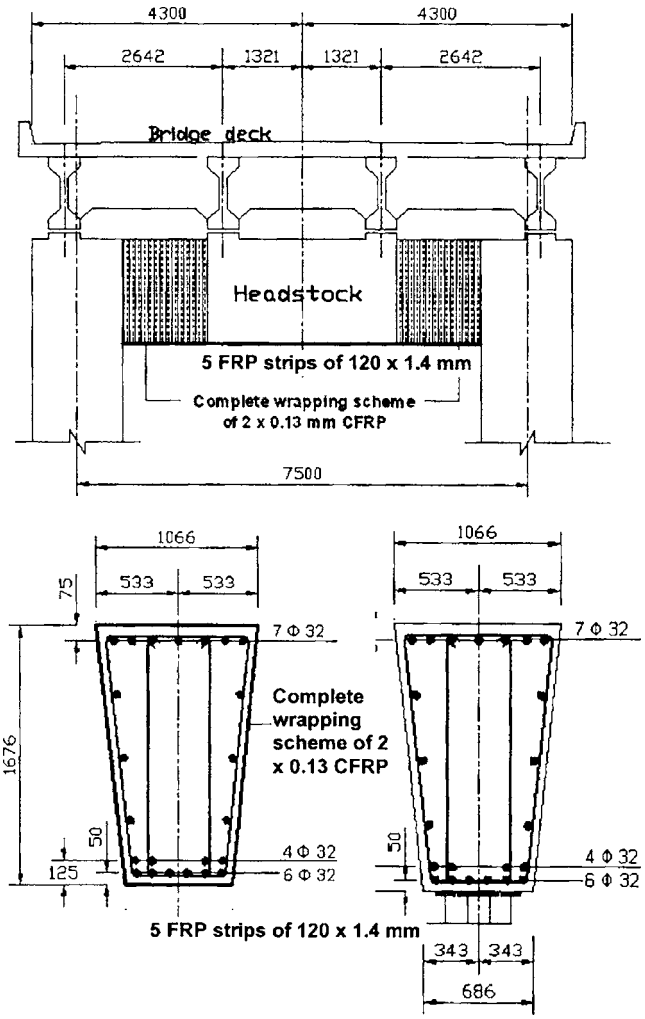

Fig. 11. Strengthening scheme

$$\varepsilon_{fe} = 0.004 \leqslant 0.75\varepsilon_{fu} \tag{31}$$

$$A_{fv} = 2nt_fw_f \tag{32}$$

where ε_{fe}=effective design value of FRP strain; ε_{fu}=ultimate strain of FRP; f_{fe}=effective design value of FRP stress for shear; A_{fv}=total area of FRP shear reinforcement; S_f=maximum spacing of FRP; α=angle between FRP principal fiber orientation and longitudinal axis of member; and d_f=depth of FRP flexural reinforcement. The FIB guideline uses the model of Triantafillou (1998) and Täljsten (1999a, b), the external FRP reinforcement may then be treated in analogy to the internal steel (accepting that the FRP carries only normal stresses in the principal FRP material direction), assuming that at the ultimate limit state in shear (concrete diagonal tension) the FRP develops an effective strain in the principal material direction. The effective strain is, in general, less than the tensile failure strain, f_u. Hence, the shear capacity of a strengthened element may be calculated according to the European Code EC2 format as follows:

$$V_{Rd} = V_{uc} + V_{us} + V_{\text{frp}} \tag{33}$$

The FRP contribution to shear capacity, V_{frp}, can be written in the following form (CEB-FIB 2002):

$$V_{\text{frp}} = 0.9\varepsilon_{fd,e}E_f\rho_f b_w d_f(\cot\theta + \cot\alpha)\sin\alpha \tag{34}$$

$$\rho_f = 2t_f \sin\alpha / b_w \tag{35}$$

$$\varepsilon_{f,e} = 0.048\left(\frac{f_{cm}^{2/3}}{E_f \rho_f}\right)^{0.47} \varepsilon_{fu} \tag{36}$$

$$\varepsilon_{fk,e} = k\varepsilon_{f,e} \tag{37}$$

$$\varepsilon_{fd,e} = \varepsilon_{fk,e}/\gamma_f \tag{38}$$

where $\varepsilon_{fd,e}$=design value of effective FRP strain; b_w=minimum width of cross section over the effective depth; d=effective depth of cross section; ρ_f=FRP reinforcement ratio; E_f=elastic modulus of FRP in the principal fiber orientation; θ=angle of diagonal crack with respect to the member axis, assumed equal to 45°; α=angle between principal fiber orientation and longitudinal axis of member; k=reduction factor equal to 0.8; γ_f=partial safety factor for FRP; and f_{cm}=mean value of the concrete compressive strength.

Use of CFRP wrapping system increases the design shear capacity of 2,065 kN for the existing member by 456 and 657 kN based on the FIB and ACI design guidelines, respectively. The results indicated that both the guidelines predicted an adequate shear capacity using the complete wrapping scheme for strengthening of the beam. The FIB shear strength prediction seems to be more conservative but the ACI formulation is more adoptable with Australian standards. The whole wrapping around the section was used, hence the CFRP shear reinforcement is not considered as contact critical shear reinforcement and the ultimate failure does not occur with debonding.

Other Design Considerations and Environmental Effects

The ACI guideline suggests imposing reasonable strengthening limits to guard the strengthened member against failure of the FRP strengthening system and collapse of the structure due to fire, vandalism, or other causes. It is recommended that the existing strength of the structure be sufficient to a level of load as described by

$$(\phi R_n)_{\text{existing}} \geq (1.25_{\text{DL}} + 0.85S_{\text{LL}})_{\text{new}} \tag{39}$$

where S_{DL}=effects of dead load and S_{LL}=effects of live load. It is also recommended that the strength of a structural member with a fire-resistance rating before strengthening should satisfy the conditions of

$$(R_{n\theta})_{\text{existing}} \geq S_{\text{DL}} + S_{\text{LL}} \tag{40}$$

where $(R_{n\theta})_{\text{existing}}$=nominal resistance of the member at an elevated temperature, which can be determined using the ACI 216R 1999 guideline. Environmental conditions affect the performances of the FRP system. The mechanical properties of FRP systems degrade under exposure to certain environments, such as alkalinity, salt water, chemicals, ultraviolet light, high temperatures, high humidity, and freezing and thawing cycles. The ACI guideline accounts for this degradation using the environmental reduction factor for the design material properties of CFRP as described earlier.

The FIB guideline recommends the accident design verification procedure to prevent failure of the FRP strengthening system and collapse of the structure due to fire, vandalism, or other causes. The existing member is subjected to all relevant accidental load combinations of the strengthened member. The verification is the performance in the ultimate limit state, considering the partial safety factors of 1.0 and considering partial safety coefficients and combination factors using Eurocode 1 (EC1), Part 1 (CEN 1994). The FIB guideline also recommends that sufficient attention should be paid to the special design aspects such as environmental conditions, cyclic loading, and extra bond stresses due to the difference in thermal expansion between FRP and concrete, impact and fire resistance may also be relevant, as they can have a considerable influence on the structural safety. The existing structural strength of the headstock was checked to be sufficient to satisfy the ACI and FIB guidelines requirements in the accidental design situation. The existing structure has not been rated for fire resistance; hence it was not checked with the requirement of Eq. (40).

Table 6. Summary of the Strengthening Calculations

Strengthening	Existing capacity	Target capacity	Strengthened beam capacity	
			ACI 440	FIB 14
Flexural (kN m)	3,840	5,320	5,392	5,809
Shear (kN)	2,065	2,520	2,722	2,521
Anchorage			Strain limitation	End anchorage Intermediate debonding End shear debonding

Summary of Strengthening Scheme

The design of the FRP strengthening system for the Tenthill Bridge headstock can be summarized as follows (see Table 6):

- The flexural strength of the beam at midspan can be increased from 3,800 to 5,392 kN m by bonding four FRP unidirectional strips of 120×1.4 mm to the tension face of the beam section (bottom fiber) with fibers oriented along the length of the member (Fig. 11).
- The shear strength of the headstock can be increased from 2,065 to 2,722 kN by complete wrapping of the beam with two layers of 0.13 mm thick carbon fibers oriented along the transverse axis of the beam section (Fig. 11).

The average width of the beam section was used for capacity analysis of existing and strengthened member.

Conclusions

A comparison between the recommendations of two design guidelines: ACI 440 and the FIB 14 in the design of externally bonded FRP systems to strengthen reinforced concrete beams in flexure and shear have been presented. The FRP type used was carbon fiber-reinforced polymer in laminate and strip form readily available in Australia. The comparison was presented using a case study of a bridge headstock: Tenthill Creek, Queensland Australia. The following conclusions can be drawn from the design calculations and the comparison.

- Both design guidelines adopt the same principle of design to estimate shear and flexural capacity enhancements of the strengthened member when applied in accordance with the guidelines of the Austroads Bridge Design Code (1992).
- The ACI guideline is more conservative in prediction of flexural capacity enhancement for the strengthened headstock.

This is mainly due to the use of an additional strength reduction factor of 0.85 applied to the contribution of FRP reinforcement in the ACI calculations and higher concrete allowable strain of 0.0035 used in the FIB calculations.
- The FIB guideline uses a more involved approach to check debonding of FRP laminates from the concrete substrate, which covers all possible bond failure modes. Alignment of the design method with Austroads, 1992 recommendations will require further work.
- The FIB shear strength prediction seems to be more conservative but the ACI formulation is more adoptable with Australian standards.

In view of the previous findings, it may be concluded that the use of ACI 440 design guideline may be more appropriate for FRP strengthening applications in Australia. The design concepts and philosophy used by ACI is similar to those adopted by AS3600 (2002). However, in considering the failure of FRP composites in debonding and anchorage zones, use of the FIB appears to be more appropriate as it systematically covers all possible scenarios. A methodology needs to be developed to align the design procedure with the Austroads (1992) provisions. The use of CFRP laminate and CFRP wrapping appears to be an effective way to strengthen the Tenthill Bridge to provide additional flexural and shear capacities. The proposed strengthening scheme for the bridge using FRP technology can be used as a basis for the development of a decision support tool for rehabilitation of reinforced concrete bridge structures using fiber-reinforced polymer composites. Through the case study an appropriate design basis for use FRP in strengthening has been developed complying with the Austroads Bridge Design Code (1992) and in accordance with the ACI-440 design guideline.

Appendix. Design Calculations

The initial strain distribution of the headstock was calculated based on structural analysis for service loading condition, long-term modulus of elasticity and the cracked section. As the service bending moment is typically greater than the cracking moment, the calculation is based on a cracked section:

$$x_0 = 250 \text{ mm} \Rightarrow \varepsilon_{c0} = \frac{M_0 x_0}{E_c I_{c0}} = \frac{2{,}758 \times 10^6 \times 250}{13{,}050 \times I_{c0}}$$

$$I_{c0} = 4.5 \times 10^9 + (15.32 - 1) \times 5{,}521 \times (250 - 75)^2 + 15.32 \times 8{,}030 \times 1{,}350^2$$

$$= 2.31 \times 10^{11} \Rightarrow \varepsilon_{c0} = \frac{M_0 x_0}{E_c I_{c0}} = \frac{2{,}758 \times 10^6 \times 250}{13{,}050 \times I_{c0}}$$

$$= 0.00023 \Rightarrow \varepsilon_0 = \varepsilon_{c0}\frac{h - x_0}{x_0} = 0.00023 \times \frac{1{,}676 - 250}{250} = 0.0013$$

Capacity of Strengthened Beam

The cross-sectional analysis indicated that the failure mode of the beam section of the headstock would be the yielding of the longitudinal steel reinforcement followed by concrete crushing, while the FRP is intact. The section design for failure mode of yielding steel followed by concrete crushing

$$f_c' = 21 \text{ MPa}$$

$$\beta_1 = 1.09 - 0.008 f_c' = 0.92 \quad \text{(ACI 1999, Section 10.2.7.3)}$$

$$E_c = 57{,}000\sqrt{f_c'} = 261{,}000$$

$$\rho_{s1} \equiv \frac{A_s}{bd} = \frac{8{,}030}{1{,}676 \times 876} = 0.0055$$

$$\rho_{s2} \equiv \frac{A_s}{bd} = \frac{5{,}521}{1{,}676 \times 876} = 0.0038$$

$$\rho_f \equiv \frac{A_f}{bd} = \frac{840}{1{,}676 \times 876} = 0.00057$$

$$nE_f t_f = 165{,}000 \times 1.4 = 231{,}000 > 180{,}000$$

$$\kappa_m = \frac{1}{60\varepsilon_{fu}}\left(\frac{90{,}000}{nE_f t_f}\right) = \frac{1}{60 \times 0.01445}\left(\frac{90{,}000}{231{,}000}\right) = 0.45 < 0.9$$

$$\varepsilon_f = \varepsilon_{cu}\frac{h - x}{x} - \varepsilon_0$$

$$\varepsilon_{s2} = \varepsilon_{cu}\frac{x - d_2}{x}$$

$$x = \frac{A_{s1} f_{sy} + A_f E_f \varepsilon_f - A_{s2} E_s \varepsilon_{s2}}{\gamma f_c' \beta_1 b}$$

$$x = 270 \text{ mm}, \quad \varepsilon_f = 0.0065 \leqslant 0.45 \times 0.01445 = 0.0065, \quad \varepsilon_{s2} = 0.00108$$

$$\phi M_n = 0.9\left[A_{s2} E_s \varepsilon_{s2}\left(\frac{\beta_1 x}{2} - d_2\right) + A_{s1} f_{sy}\left(d - \frac{\beta_1 x}{2}\right) + \psi A_f E_f \varepsilon_f \left(h - \frac{\beta_1 x}{2}\right)\right]$$

$$\phi M_n = 0.9\begin{bmatrix} 5{,}621 \times 200{,}000 \times 0.00108(123 - 75) + 8{,}030 \times 400(1{,}600 - 123) \\ + 0.85 \times 840 \times 165{,}000 \times 0.0065 \times (1{,}676 - 123) \end{bmatrix} = 5{,}932 \text{ kN m}$$

Flexural strength based on FIB14: Calculation of neutral axis depth, x:

$$0.85\psi f_{cd} b x + A_{s2} E_s \varepsilon_{s2} = A_{s1} f_{yd} + A_f E_f \varepsilon_f$$

Try use of 4 FRP strips of 120×1.4

$$0.85 \times 0.8 \times \frac{21}{1.5} \times 876x + 5{,}621 \times 200{,}000\varepsilon_{s2} = 8{,}030 \times \frac{400}{1.15} + 672 \times 165{,}000\varepsilon_f$$

$$\varepsilon_f = \varepsilon_{cu}\frac{h-x}{x} - \varepsilon_0$$

$$\varepsilon_{s2} = \varepsilon_{cu}\frac{x-d_2}{x}$$

$$x = 282 \text{ mm}, \quad \varepsilon_f = 0.0074 < 0.0126, \quad \varepsilon_{s2} = 0.0012$$

$$M_{\mathrm{RD}} = A_{s2}E_s\varepsilon_{s2}(\delta_G x - d_2) + A_{s1}f_{yd}(d - \delta_G x) + A_f E_{fu}\varepsilon_f(h - \delta_G x)$$

$$M_{\mathrm{RD}} = 5{,}621 \times 200{,}000 \times 0.0012(0.4 \times 282 - 75) + 8030\frac{400}{1.15}(1{,}600 - 0.4 \times 282) + 840 \times 165{,}000 \times 0.0074 \times (1{,}676 - 0.4 \times 282) = 5{,}809 \text{ kN m}$$

Anchorage

The ACI user guide place a limitation on the strain level in the laminate to prevent delamination of FRP from the concrete substrate.

$$nE_f t_f = 165{,}000 \times 1.4 = 231{,}000 > 180{,}000$$

$$\kappa_m = \frac{1}{60\varepsilon_{fu}}\left(\frac{900{,}00}{nE_f t_f}\right) = \frac{1}{60 \times 0.01445}\left(\frac{90{,}000}{231{,}000}\right) = 0.45 < 0.9$$

$$\varepsilon_f = \varepsilon_{cu}\frac{h-x}{x} - \varepsilon_0 = 0.0065 \leqslant \kappa_m\varepsilon_{fu} = 0.45 \times 0.01445 = 0.0065$$

The FIB guideline: Approach 1: Verification of end anchorage, Strain limitation in the FRP reinforcement:

$$N_{fa,\max} = \alpha c_1 k_c k_b b\sqrt{E_f t_f f_{ctm}} \text{ (N)}$$

$$l_{b,\max} = \sqrt{\frac{E_f t_f}{c_2 f_{ctm}}} \text{ (mm)}$$

$$l_{b,\max} = \sqrt{\frac{165{,}000 \times 1.4}{2 \times 2}} = 240 \text{ mm}$$

$$k_b = 1.06\sqrt{\frac{2 - \frac{b_f}{b}}{1 + \frac{b_f}{400}}} = 1.06\sqrt{\frac{2 - \frac{600}{686}}{1 + \frac{600}{400}}} = 0.71 < 1$$

$$N_{fa,\max} = \alpha c_1 k_c k_b b_f\sqrt{E_f t_f f_{ctm}} = 0.9 \times 0.64 \times 1.0 \times 1.0 \times 600\sqrt{165{,}000 \times 1.4 \times 2} = 235 \text{ kN}$$

Theoretical cutoff point

$$N_{fa,\max} = \frac{M\alpha_f A_f(h-x)}{I_{cs}}$$

$$235{,}000 = \frac{M \times 12.64 \times 840(1{,}676 - 282)}{2.51 \times 10^{11}} \Rightarrow M = 3{,}985 \text{ kN m}$$

Provided anchorage length = 1,000 mm > $l_{b,\max}$ = 240 mm (required).

Approach 2: Calculation of the envelope line of tensile stress: Determination of the most unfavorable spacing of flexural cracks,

$$\tau_{sm} = 1.85f_{ctm} = 1.85 \times 2 = 3.70$$

$$\tau_{fm} = 0.44f_{ctm} = 0.44 \times 2 = 0.88$$

$$s_{rm} = 2l_t = 2\frac{M_{\mathrm{cr}}}{z_m}\frac{1}{(\sum \tau_{sm}b_f + \sum \tau_{sm}d_s\pi)} = 478 \text{ mm}$$

$$\max \Delta\sigma_{fd} = \frac{c_1}{\gamma_c}\sqrt{\frac{E_f\sqrt{f_{ck}f_{ctm}}}{t_f}} = \frac{0.23}{1.5}\sqrt{\frac{165{,}000\sqrt{21 \times 2}}{1.4}} = 134 \text{ MPa}$$

$$l_{b,\max} = c_2\sqrt{\frac{E_f t_f}{\sqrt{f_{ck}f_{ctm}}}} = 1.44\sqrt{\frac{165{,}000 \times 1.4}{\sqrt{21 \times 2}}} = 210 \text{ mm}$$

$$\max \Delta\sigma_{fd} = 134 \text{ MPa} > \Delta\sigma_{fd} = 105 \text{ MPa}$$

Approach 3: Verification of anchorage and the force transfer between FRP and concrete:

$$f_{cbd} = 1.8\frac{f_{ctk}}{\gamma_c} = 1.8\frac{2}{1.5} = 2.4 \text{ MPa}$$

$$\varepsilon_{s1} < \varepsilon_{yd}: \quad \frac{V_d}{0.95db_f\left(1 + \frac{A_{s1}E_s}{A_f E_f}\right)} = 0.17 < f_{cbd}$$

$$\varepsilon_{s1} \geqslant \varepsilon_{yd}: \quad \frac{V_d}{\frac{z_s + z_f}{2}b_f} = 2.1 < f_{cbd}$$

Shear Strengthening

In accordance with ACI the shear strength may be calculated as follows:

$$\phi V_n = \phi(V_{uc} + V_{us} + \psi_f V_{\mathrm{frp}})$$

$$\varepsilon_{fe} = 0.004 \leqslant 0.75\varepsilon_{fu}$$

$$\varepsilon_{fe} = 0.004 < 0.75 \times 0.01275 = 0.009$$

$$f_{fe} = \varepsilon_{fe}E_f = 0.004 \times 230{,}000 = 920 \text{ MPa}$$

$$A_{fv} = 2nt_f w_f = 2 \times 2 \times 0.13 \times 1{,}676 = 871 \text{ mm}^2$$

$$V_{\text{frp}} = \frac{A_{fv} f_{fe} (\sin\alpha + \cos\alpha) d_f}{S_f} = 871 \times 920(1) = 801 \text{ kN}$$

$$\phi V_n = V_{\text{existing}} + \phi(\psi_f V_{\text{frp}}) = 2{,}075 + 0.85(0.95 \times 801) = 2{,}796 \text{ kN}$$

The shear capacity of a strengthened element may be calculated according to the EC2 format and the FIB guideline as follows:

$$V_{\text{Rd}} = (\phi V_{uc} + \phi V_{us} + V_{\text{frp}})$$

The FRP contribution to shear capacity, V_{frp}, can be written in the following form:

$$\rho_f = 2t_f \sin\alpha / b_w = 2 \times 0.13(2)/876 = 0.0006$$

$$\varepsilon_{f,e} = 0.048\left(\frac{f_{cm}^{2/3}}{E_{fu}\rho_f}\right)^{0.47},$$

$$\varepsilon_{fu} = 0.048\left(\frac{21^{2/3}}{230{,}000 \times 0.006}\right)^{0.47} = 0.0042$$

$$\varepsilon_{fk,e} = k\varepsilon_{f,e} = 0.8 \times 0.0042 = 0.0034$$

$$\varepsilon_{fd,e} = \varepsilon_{fk,e}/\gamma_f = 0.003/1.35 = 0.0025$$

$$V_{\text{frp}} = 0.9\varepsilon_{fd,e} E_f \rho_f b_w d(\cot\theta + \cot\alpha)\sin\alpha = 456 \text{ kN}$$

$$V_{\text{Rd}} = (V_{\text{existing}} + V_f) = (2{,}057 + 456) = 2{,}521 \text{ kN}$$

Notation

The following symbols are used in this paper:

A = cross-sectional area of a member (mm^2);
A_f = total area of FRP reinforcement (mm^2);
A_{fv} = total area of FRP shear reinforcement (mm^2);
A_s = area of nonprestress reinforcement (mm^2);
A_{st} = total area of longitudinal reinforcement (mm^2);
A_{s1} = total area of tensile longitudinal reinforcement (mm^2);
A_{s2} = total area of compressive longitudinal reinforcement (mm^2);
b = average width at the cross section (mm);
b_f = width of FRP reinforcement (mm);
b_w = web width of diameter of circular section (mm);
C_E = environmental reduction factors;
d_s = diameter of steel reinforcement (mm);
d_0 = distance from extreme compression fiber to the centroid of the nonprestresses steel tension reinforcement (mm);
E_c = modulus of elasticity of the concrete (MPa);
E_f = modulus of elasticity of FRP (MPa);
E_s = modulus of elasticity of reinforcement steel (MPa);
f'_c = specified compressive strength of concrete (MPa);
f_{cbd} = design bond shear strength of concrete (MPa);
f_{ck} = characteristic value of the concrete compressive strength (MPa);
f_{ctk} = characteristic value of the concrete tensile strength (MPa);
f_{ctm} = mean value of the concrete tensile strength (MPa);
f_{fe} = effective stress in the FRP reinforcement (MPa);
f_{fu} = FRP ultimate tensile strength (MPa);
h = total depth of the member;
I = second moment area of a member (mm^4);
I_{cs} = moment of inertia of transformed cracked section after strengthening (mm^4);
k = ratio of the depth of the neutral axis to the reinforcement depth in elastic analysis of the cross section;
k_b = size factor;
k_c = concrete compaction factor;
k_1 = modification factor applied to κ_v to account for the concrete strength;
k_2 = modification factor applied to κ_v to account for the wrapping scheme;
L_e = active bond length of FRP laminate;
l_b = bond length;
$l_{b,\max}$ = maximum anchorage length;
l_t = transmission length;
M^* = applied moment at the section (kN m);
$\max \Delta\sigma_{fd}$ = design value of maximum possible increase in FRP tensile stress between two subsequent cracks (MPa);
M_{cr} = cracking moment;
M_{Rd} = resisting design moment (kN m) FIB 14, 2002;
M_u = nominal design flexural strength (kN m);
M_0 = acting moment during strengthening (kN-m);
N_f = force in FRP;
n = number of FRP reinforcement piles;
$N_{fa,\max}$ = maximum anchorable force;
N_{s1} = force in tensile steel reinforcement;
R_n = nominal strength of member;
$R_{n\theta}$ = nominal strength of member subjected to the elevated temperature associated with a fire;
S_{DL} = dead load effect;
S_{LL} = live load effect;
s_f = maximum spacing of FRP;
s_{rm} = mean value of crack spacing;
t_f = nominal thickness of the FRP reinforcement (mm);
V_{frp} = nominal shear strength provided by FRP reinforcement (N);
V_n = applied shear force at the section (kN);
V_u = nominal shear strength of a member (N);
V_{uc} = nominal shear strength provided by concrete with steel flexural reinforcement (N);
V_{us} = nominal shear strength provided by steel stirrups (N);
w_f = width of FRP reinforcing plies (mm);
x = depth of the compression zone;
z_f = mean lever arm of internal forces to the FRP reinforcement;
z_m = mean lever arm of internal forces;
z_s = mean lever arm of internal forces to the steel reinforcement;
α = reduction factor to account for the influence of inclined cracks on the bond strength;
α_f = modular ratio for nonprestressed steel;
β = coefficient with or without numerical subscript;
ε_{cu} = ultimate concrete strain;
ε_f = FRP strain;
ε_{fe} = effective design value of FRP strain;
ε_{fu} = FRP ultimate strain;

ε_s = strain in steel reinforcement;
ε_{s1} = tensile steel strain;
ε_y = yield strain of the steel reinforcement;
ε_{yd} = design value of the yield strain of the steel reinforcement;
ε_o = initial concrete strain in the extreme compressive fiber before strengthening, or unconfined concrete strain at peak stress;
ε_0 = initial strain at the extreme tensile fiber before strengthening;
ϕ = strength-reduction factor;
γ = multiplier to determine the intensity of an equivalent rectangular stress distribution for concrete;
κ_m = bond dependent coefficient for flexure;
ρ_f = FRP reinforcement ratio;
ρ_{s1} = ratio of nonprestressed tensile reinforcement;
ρ_{s2} = ratio of nonprestressed compressive reinforcement;
σ_f = FRP tensile stress;
σ_{fad} = design value of FRP tensile stress at the end anchorage (MPa);
$\sigma_{fad,\max}$ = design value of maximum anchrable FRP tensile stress (MPa);
σ_{fd} = design value of FRP tensile stress;
τ_{fm} = mean bond stress of the FRP;
τ_{sm} = mean bond stress of the steel reinforcement; and
ψ_f = FRP strength reduction factor.

References

American Concrete Institute (ACI). (1999). "Guide for determining the fire endurance of concrete elements." *ACI 216R*, Farmington Hills, Mich.

American Concrete Institute (ACI). (1999). "Building code requirements for structural concrete and commentary." *ACI 318-99*, Farmington Hills, Mich.

American Concrete Institute (ACI). (2003). *Guide for the design and construction of externally bonded FRP systems for strengthening concrete structures*, American Concrete Institute Committee 440, Farmington Hills, Mich.

Australian Standard (AS). (2002). "Concrete structures." *AS3600*, Standards Association, Canberra, Australia.

Austroads (1992). *Bridge design code*, *Section 2: Design loads*, Canberra, Australia.

Bakht, B., et al. (2000). "Canadian bridge design code provisions for fiber-reinforced structures." *J. Compos. Constr.*, 4(1), 3–15.

Bakis, C. E., Bank, L. C., Brown, V. L., Cosenza, E., Davalos, J. F., Lesko, J. J., Machida, A., Rizkalla, S. H., and Triantifillou, T. C. (2002). "Fiber-reinforced polymer composites for construction-state-of-the-art review." *J. Compos. Constr.*, 6(2), 73–87.

Comité Européen de Normalisation (CEN). (1994). "Eurocode 1: Basis of design and actions on structures—Part 1: Basis of design." *ENV 1991-1*, Brussels, Belgium.

CSi Products. (2003). "Integrated software for structural analysis and design." *SAP 2000*. *Computers and structures*, Berkeley, Calif.

Fenwick, J. M., and Rotolone, P. (2003). "Risk management to ensure long term performance in civil infrastructure." *21st Biennial Conf. of the Concrete Institute of Australia*, Brisbane, Australia, 647–656.

Holzenkämpfer, P. (1994). "Ingenieurmodelle des verbundes geklebter bewehrung für betonbauteile." Dissertation, TU Braunschweig, München, Germany (in German).

Japan Society of Civil Engineers (JSCE). (1997). "Recommendations for design and construction of concrete structures using continuous fiber reinforcing materials." *Concrete engineering series 23*, A. Machinda, ed., Tokyo.

Kalra, R., and Neubauer, U. (2003). "Strengthening of the Westgate Bridge with carbon fibre composites—A proof engineer's perspective." *21st Biennial Conf. of the Concrete Institute of Australia*, Brisbane, Australia, 245–254.

Neubauer, U., and Rostásy, F. S. (1997). "Design aspects of concrete structures strengthened with externally bonded CFRP-plates." *Concrete+Composites, Proc., 7th Int. Conf. on Structural Faults and Repair*, Vol. 2, 109–118.

Nezamian, A., and Setunge, S. (2004a). "Comparison between ACI 440 and FIB 14 design guidelines in using CFRP for strengthening of s concrete bridge headstock." *Proc., 4th Int. Conf. on Advanced Composite Materials in Bridges and Structures*, Calgary, Alta., Canada.

Nezamian, A., Setunge, S., Kumar, A., and Fenwick, J. M. (2004b). "Decision support in using fiber reinforced polymer (FRP) composites in rehabilitation of concrete bridge structures." *Proc., of Innovative Materials and Technologies for Construction and Restoration*, Lecce, Italy.

Niedermeier, R. (2000), "Zugkraftdeckung bei klebearmierten bauteilen (Envelope line of tensile forces while using externally bonded reinforcement)." Doctoral dissertation, TU München, Germany (in German).

Nystrom, H. E., Walkins, S. E., Nanni, A., and Murray, S. (2003). "Financial viability of fiber-reinforced polymer (FRP) bridges." *J. Manage. Eng.*, 19(1), 2–8.

Pantelides, C. P., Alameddine, F., Sardo, T., and Imbsen, R. (2004a). "Seismic retrofit of state street bridge on Interstate 80." *J. Bridge Eng.*, 9(4), 333–342.

Pantelides, C. P., Cercone, L., and Policelli, F. (2004b). "Development of a specification for bridge seismic retrofit with carbon fiber-reinforced polymer composites." *J. Compos. Constr.*, 8(1), 88–96.

Policelli, F. (1995). "Carbon fiber jacket wrapping of five columns on the Santa Monica Viaduct, Interstate 10, Los Angeles." *Structural Systems Research Rep. ACTT/BIR-95/14*, Univ. of California at San Diego, La Jolla, Calif.

Seible, F., Hegemeir, G., Policelli, F., Karbhari, V., Randolph, R., and Belknap, F. (1995). "Earthquake retrofit of bridge columns with continuious fiber jacket." *Advanced Composite Technology Transfer Consortium/Bridge Infrastructure Renewal Rep. ACTT-95-07*, DARPA, Univ. of California at San Diego, La Jolla, Calif., I–IV.

Shahrooz, B. M., and Boy, S. (2004). "Retrofit of a three-span slab bridge with fiber-reinforced polymer systems—Testing and rating." *J. Compos. Constr.*, 8(3), 241–247.

Shepherd, B., and Sarkady, A. (2002). "Carbon fibre fabric strengthening of Little River Bridge." *Proc., IABSE Symp.*, Melbourne Australia.

Sika Australia Pty Limited. (2004). "Heavy duty CFRP strengthening system." *Product guide specification*, Melbourne, Australia, ⟨http://www.sika.com.au⟩

Täljsten, B. (1999a), "Förstärkning av befintliga betongkonstruktioner med kolfiberväv eller laminat, Dimensionering, material och utförande." *Technical Rep. 1999:12*, Lulea Univ. of Technology, Lulea, Sweden (in Swedish).

Täljsten, B. (1999b). "Strengthening of existing concrete structures with carbon fibre fabrics or laminates. Design, material, and execution." *Extract*, Swedish National Railroad and Road Codes, Stockholm, Sweden.

The International Federation for Structural Concrete (CEB-FIB). (2002). "Externally bonded FRP reinforcement for RC structures." *Technical Rep. Bulletin No. 14*, ⟨Lausanne, Switzerland, www.fib-international.org⟩.

Triantafillou, T. C. (1998). "Shear strengthening of reinforced concrete beams using epoxy bonded FRP composites." *ACI Struct. J.*, 95(2), 107–115.